ELSEVIER

Journal of Chromatography B, 769 (2002) 97–106

JOURNAL OF CHROMATOGRAPHY B

www.elsevier.com/locate/chromb

Detection of doxorubicin and metabolites in cell extracts and in single cells by capillary electrophoresis with laser-induced fluorescence detection

Adrian B. Anderson, Jamie Gergen, Edgar A. Arriaga*

Department of Chemistry, University of Minnesota, 207 Pleasant Street SE, Minneapolis, MN 55455, USA

Received 9 August 2001; received in revised form 5 December 2001; accepted 17 December 2001

Abstract

Capillary electrophoresis with laser-induced fluorescence detection was used to separate and detect doxorubicin and at least five metabolites from NS-1 cells that were treated with 25 μ*M* doxorubicin for 8 h. Using 10 m*M* borate, 10 m*M* sodium dodecyl sulfate (pH 9.3) as separation buffer, the 488-nm argon-ion laser line for fluorescence excitation, and a 635±27.5 nm bandpass filter for detection, the limit of detection ($S/N=3$) for doxorubicin is 61±13 zmol. This low limit of detection allows for the detection of a larger number of metabolites than previously reported. Two extraction procedures were performed: a bulk liquid–liquid extraction and an in-capillary single-cell lysis. While in the bulk liquid–liquid extraction procedure, recovery for doxorubicin range from 50 to 99%, in single cell analysis the recovery is expected to be complete. Furthermore performing lysis of a single cell inside the separation capillary prevents doxorubicin or metabolite loss or degradation during handling. Based on the bulk method the calculated metabolite abundance is in the sub-amol per cell range while it varies from 0.1 to 1.1 fmol per cell in single cell analysis confirming metabolite loss during handling. Each metabolite was found at a level less than 0.1% of the doxorubicin content in either method, suggesting a slow metabolism in the NS-1 cell system or effective removal of metabolites by the cell.

Keywords: Doxorubicin

1. Introduction

Doxorubicin (DOX) is a widely used anthracycline that has proven to be effective against a variety of human malignancies [1], such as leukemia and breast cancer [2]. When this drug reaches the targeted organ as free drug administered intravenously or encapsulated in liposomes [3,4] it enters the malignant cells, reaches their nuclei, and stabilizes the topoisomerase IIα–DNA complex, halting cell proliferation [5]. This process is believed to be the main mechanism of action. Unfortunately, the DOX treatment is accompanied by the appearance of cardiac and liver toxicity [6–9] and drug resistance [6,10,11] which may result from cellular processes involving the parent compound or drug metabolites [12,13]. Furthermore, transformation of DOX into metabolites, which may not be pharmacologically active, decreases the concentration of the parent compound affecting the efficacy of the treatment.

*Corresponding author. Tel.: +1-612-624-8024; fax: +1-612-626-7541.

E-mail address: arriaga@chem.umn.edu (E.A. Arriaga).

1570-0232/02/$ – see front matter
PII: S1570-0232(01)00633-X

Therefore, it is important to design sensitive analytical procedures that can detect the various metabolites that may be present in the cell after DOX treatment.

DOX metabolism has been studied previously [12–14]. Based on the DOX metabolic scheme proposed by Licata et al. [13] the expected metabolites are shown in Fig. 1. This work was based on the in vitro incubation of the parent compound with human cardiac cytosol. Andersen et al. reported five metabolites [14]. Since most of the cytotoxic activity of DOX is derived from the aglycone ring system of the molecule [1,12], those metabolites that retain this molecular feature are expected to be toxic. In order to fully explain the role that DOX metabolites play in its mechanism of action, unwanted cytotoxicity, and appearance of drug resistance it is necessary to develop direct methods that are capable of extracting, separating, and detecting doxorubicin metabolites. Some of these methods are discussed below.

The most common methods for extraction of DOX are solid-phase extraction [15–17], enzymatic digestion of cellular material [14], and liquid–liquid extraction (LLE) [6,18,19]. In the liquid–liquid extraction procedures reported in the literature, a biological sample is treated with chloroform or a chloroform/alcohol mixture in order to lyse the cells and extract the DOX into the organic phase. The phases are separated and the organic phase is dried under a steady stream of nitrogen.

Following the extraction by any of the procedures

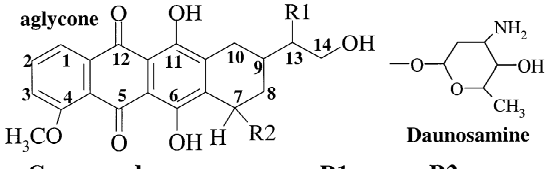

Compound	R1	R2
Doxorubicin	O	Daunosamine
Doxorubicinol	OH	Daunosamine
Doxorubicin hydroxyaglycone	O	OH
Doxorubicinol hydroxyaglycone	OH	OH
Doxorubicin aglycone	O	H

Fig. 1. Chemical structure of doxorubicin and four previously reported metabolites [13].

mentioned above, anthracyclines, including DOX and their metabolites are separated and commonly characterized by reversed-phase liquid chromatography [6,18,20–23]. Because anthracyclines, including DOX, and their metabolites exhibit native fluorescence due to the conjugated aglycone ring system present in the molecule, fluorescence is the preferred detection scheme. Using excitation at either 460 or 480 nm and detection at 550 nm, DOX limits of quantification in the fmol range have been reported [18,23].

Another separation technique that may be used for the analysis of anthracyclines is capillary electrophoresis (CE) with laser-induced fluorescence detection (LIF). The determination of anthracyclines including DOX by CE–LIF was done first by Reinhoud et al. [24]. The limit of detection for the CE–LIF method was 24 amol, a limit of detection three orders of magnitude lower than those obtained by reversed-phase liquid chromatography analyses. Recently the CE separation of a mixture of anthracyclines containing DOX, daunorubicin, and idarubicin was reported [25]. Hempel et al. have used CE–LIF for separation and quantification of parent anthracyclines and their main metabolite: idarubicin from idarubicinol and DOX from doxorubicinol in samples from plasma of patients treated with the respective drug [19,26]. Furthermore, Siméon et al. have reported the CE–LIF analysis of an anthracycline, daunorubicine, extracted from tumor biopsies [27]. However, they did not report the separation of anthracycline metabolites produced by the cells of the biopsy.

One of the unique applications of CE has been its application to the analysis of the contents of single mammalian cells [28–32]. In single cell analysis a whole cell is rapidly disrupted inside a capillary resulting in the release of all its metabolites which then can be separated by CE. This procedure eliminates the risk of metabolite degradation during a lengthy extraction procedure and guarantees complete recovery [33]. So far, metabolic studies based on single cell analysis by CE–LIF have been limited to synthetic fluorescent substrates that resemble the natural substrates [29,33,34]. Because of these structural modifications it is expected that the analysis will result in a slightly altered description of metabolism. Single-cell analysis by CE may provide an

accurate description of doxorubicin metabolism because doxorubicin is an unmodified substrate.

Here we demonstrate a sensitive CE–LIF method for the separation and detection of doxorubicin and at least five of its metabolites in bulk preparations and in single cells. Using this method, we present the most complete description of low-abundance DOX metabolites produced in vivo by cultured cells to date.

2. Experimental

2.1. Chemicals and reagents

Doxorubicin HCl (ICN, Costa Mesa, CA, USA), 13-dihydrodoxorubicin HCl (doxorubicinol) (Dr A. Suarato, Pharmacia, Nerviano, Italy), fluorescein reference standard (Molecular Probes, Eugene, OR, USA), sodium borate decahydrate (EN Science, Gibbstown, NJ, USA), sodium dodecyl sulfate (SDS) Ultrapure Bioreagent and potassium phosphate monobasic (J.T. Baker, Phillipsburg, NJ, USA), methanol (MeOH) and acetonitrile (Mallinckrodt, Paris, KY, USA), chloroform (Aldrich, Milwaukee, WI, USA), *N*-[2-hydroxyethyl]piperazine-*N′*-[2-ethane sulfonic acid] (HEPES), D-mannitol, and phosphate buffered saline (PBS) (Sigma, St. Louis, MO, USA), sucrose (Fischer, Fair Lawn, NJ, USA), ethylenediaminetetraacetic acid (EDTA) (Alfa Aesar, Ward Hall, MA, USA). Buffers for capillary electrophoresis were 10 m*M* borate–10 m*M* SDS (pH 9.3) (BS buffer), 100 m*M* phosphate (pH 4.2)–acetonitrile (7:3, v/v), and 250 m*M* sucrose–10 m*M* HEPES (pH 7.5). All buffers were made using high-performance liquid chromatography (HPLC) grade water (Mallinckrodt) that had been filtered through a 0.22 μm Nalgene filter. The pH of all solutions was adjusted with either HCl or NaOH. Following pH adjustment, buffers were filtered through a 0.22 μm Nalgene filter and stored at room temperature for up to 1 month.

A 10^{-3} *M* doxorubicin stock solution was prepared in 100% MeOH and allocated into amber polypropylene vials. The DOX stock solutions were stored at −20 °C and used up to 1 month post preparation. On the day of analysis one vial of DOX stock solution was used to prepare standard dilutions and for cell treatment. A new vial of stock DOX solution was used each day to prevent repeated thermal cycling between −20 °C and 25 °C.

2.2. Cell incubation and sample preparation

NS-1 cells were incubated at 37 °C and 5% CO_2 in Dulbecco's modified eagle medium (DMEM) (Sigma) 3 days after splitting with 25 μ*M* DOX for 8 h. The concentration of 25 μ*M* DOX was chosen because this was the maximum dosage of DOX that would maintain cell viability at 80% after treatment. Trypan Blue Solution (0.4%) (Sigma) was used to stain non-viable cells. Cell viability was then calculated as the ratio of viable cells to total cells. Following incubation, cells were divided into five 1.4 ml replicates and pelleted at 1800 *g* for 5 min using an Eppendorf microfuge (Brinkman Instruments, Inc., Westbury, NJ, USA) and washed twice in PBS. The average cell density was of $1.6\pm0.4\times10^{6}$ cells/sample as determined with a Fuchs Rosenthal ultra plane counting chamber (Hausser Scientific, Horsham, PA, USA).

2.3. Liquid–liquid extraction

Cellular membranes were dissolved and proteins denatured by adding 450 μl of BS buffer to each sample. Following addition of the BS buffer, the samples were sonicated for 1 h to enhance disruption. Following lysis, 1.05 ml of $CHCl_3$–MeOH (5:1, v/v) was added to each sample to extract doxorubicin and metabolites. The samples were subjected to two cycles of vortex mixing for 5 min to improve the extraction followed by centrifugation for 10 min at 1000 *g* to separate the layers. The less dense aqueous layer and emulsification were removed with a syringe and discarded. The samples were dried at 45 °C under a stream of nitrogen. Following drying, 100 μl of 100% MeOH was added to the vial to reconstitute the residue remaining in the sample vial. The sample was sonicated for 15 min to facilitate reconstitution.

2.4. Validation of extraction method

In a separate experiment, four replicates of each 10^{-7} *M*, 10^{-8} *M*, and 10^{-9} *M* DOX were added to

NS-1 cell lysate and then collected by an immediate recovery with the LLE procedure previously described. Following LLE of these DOX-fortified lysates, the lysates were reconstituted in BS buffer–MeOH (5:1, v/v). A control for 100% recovery was made by adding cellular extracts not containing DOX to BS buffer–MeOH (5:1, v/v) containing DOX. Based on the ratio of the DOX peak areas determined by CE–LIF for the DOX-fortified extracts and the controls we determined the recovery of the method.

2.5. CE–LIF analysis

A 10 μl aliquot of each replicate was diluted to 16.7% MeOH (v/v) with 50 μl of BS buffer prior to analysis. Fresh dilutions were done on the day of the analysis and diluted samples were not stored for reuse after more than 12 h. Each one of the five replicates was analyzed once. Sample preparations were stored at −20 °C in polypropylene vials for up to 1 month after extraction. The same preparative procedures prior to CE–LIF were observed for doxorubicin standards and controls.

Capillary electrophoresis was performed using a home-built capillary electrophoresis instrument. This instrument has been described previously [35]. Separation voltage was supplied by a CZE1000R high voltage power supply (Spellman, Hauppauge, NY, USA). The 488 nm line of an argon ion laser (Melles Griot, Carlsbad, CA, USA) was used for fluorescence excitation. Data was collected at 50 Hz using a Labview (National Instruments, Austin, TX, USA) program written in house. Samples were separated under positive polarity in a 35.0 cm uncoated fused-silica capillary with an internal diameter of 50 μm and outer diameter of 150 μm. Two millimeters of the polyimide coating was burned off at each end of the capillary.

The detector was aligned by continuously injecting 10^{-9} *M* fluorescein and maximizing the response of the photomultiplier tube (PMT) (Hamamatsu, Bridgewater, NJ, USA) by adjusting the position of the cuvette with *x*, *y* and *z* translation stages. Samples were injected electrokinetically for 5 s at 3.53 kV and then separated under 14.12 kV. Electrophoresis running buffer was BS buffer. Fluorescence detection was done using a post-column sheath flow cuvette with a 635±27.5 nm bandpass filter (Omega Optical, Brattleboro, VT, USA). A PMT biased at 1000 V was used to collect the fluorescence photons. In order to minimize migration time and peak area variations between injections during the electrophoresis it was necessary to flush the capillary with the aid of a 3 cm^3 syringe adapted to junction with the capillary. Constant pressure was applied to the syringe using a three-prong clamp for 2 min with both the methanol and water flush and then 3 min with running buffer to remove any fatty acids or proteins carried through the extraction that had adsorbed to the capillary surface. The capillary was then flushed with running buffer for 3 min prior to the subsequent analysis. The capillary was stored overnight in running buffer under constant siphoning via a height differential between the ends of the capillary.

Data plotting and analysis was performed using IGOR Pro (Wavemetrics, Lake Oswego, OR, USA). A Median filter that eliminates spikes produced by bubbles with 10-point binomial smoothing was used to process all data.

2.6. Single cell analysis

Cells are incubated as described above. In order to eliminate the DOX present in the media or excreted metabolites, which may bias single cell determinations, the cells were washed twice with sterile 210 m*M* D-mannitol–10 m*M* sucrose–5 m*M* HEPES–5 m*M* EDTA (pH 7.4) (mannitol buffer) and resuspended in the same buffer. For single cell injections a 39.5 cm fused-silica capillary (20 μm I.D.) was used. The capillary is placed in a Plexiglass holder and vertically positioned (*z*-axis) over the stage of an inverted stage microscope (Nikon, Melville, NY, USA). The Plexiglas holder is positioned in the center under 10× magnification using *x*, *y*, *z* micromanipulation translation stages (SOMA Scientific, Irvine, CA, USA). Once centered, the capillary is lowered into a 5 μl drop of cell suspension. Using the *x*–*y* translation of the microscope stage a cell is brought under the capillary image; then the capillary is micromanipulated and lowered over the cell, trapping the cell in the lumen of the capillary. The cell is injected in the capillary with a 1-s siphoning pulse applied by lowering the waste height at the

outlet of the capillary to 114 cm below the injection end. This creates a negative injection pressure of 11.2 kPa which introduces less than 0.1 nl into the capillary [29]. The capillary is then removed from the Plexiglas holder and placed in a vial containing BS buffer. A 30-s delay prior to applying separation voltage is given to allow for cell lysis [33]. Separation is done under 400 V/cm.

2.7. Fluorescence spectra

Excitation and emission spectra were obtained with a FP-6200 spectrofluorometer (Jasco, Tokyo, Japan). DOX was diluted to a concentration of 10^{-7} *M* in BS buffer for spectral analysis. The sample was placed in a 1 cm path length quartz cuvette.

3. Results and discussion

3.1. Separation and detection conditions

BS buffer was adequate for analysis of doxorubicin and its metabolites by CE–LIF. In comparison to 100 m*M* phosphate (pH 4.2)–acetonitrile (7:3, v/v) characterized by high background (1.3±0.06 V; background±SD in background), the BS buffer had a 19-fold lower background (0.0757±0.0014 V). Also, 250 m*M* sucrose–10 m*M* HEPES (pH 7.5) was tested as a running buffer. The pH of this buffer is near the pK_a of the amine group (7.5) of the daunosamine sugar (group R2 in Fig. 1) [36], thus leading to electrostatic interaction with the silanol groups on the capillary wall. Although DOX was detected using this buffer, extreme tailing of the DOX signal was observed. Because the BS buffer has a pH of 9.3, which is two orders of magnitude higher than the pK_a for the amino group, the daunosamine sugar is mostly deprotonated and neutral. Also, at this pH a large fraction of the silanol groups are deprotonated implying that electrostatic interactions with the capillary wall are reduced. Further reduction of wall interactions results from the affinity between DOX and SDS micelles in this separation buffer [37], which further competes with the interactions between DOX and the capillary walls. Therefore the BS buffer was chosen as the running buffer for the experiments described below.

In order to determine adequate settings for fluorescence detection of low abundance metabolites, we measured the excitation and emission spectra for DOX in BS buffer (Fig. 2). The excitation maximum is at 500 nm and there are two emission maxima at 550 and 580 nm. Overlaying of the emission profile with the transmission profiles for the tested bandpass filters, 530±25, 580±15 and 635±27 nm, allowed us to identify the filter that provides optimum fluorescence collection and scattering rejection (Table 1). Although the 580±15 nm filter is expected to be the best option in transmitting fluorescence, (Fig. 2B and Table 1), this filter also transmits water Raman bands present over the range of 565–599 nm [38]. As expected, electropherograms obtained when using this filter have the highest background of the three filters that were evaluated (Table 1). We also tested the 530±25 nm filter because (Table 1) it was expected to provide a good signal-to-noise (S/N) ratio due to its transmission range. Unfortunately, this filter seems to transmit 488-nm radiation caused by Raleigh scattering or fluorescence from contaminants that may be found in the BS buffer. The best S/N ratio was observed when using the 635 nm filter which coincides with the best limit of detection ($S/N = 3$), 61±13 zmol. This mass limit of detection (LOD) is three orders of magnitude lower than any other mass limit of detection previously reported [24]. Therefore, selecting the 635 filter was considered adequate for analysis of DOX and low abundance metabolites.

3.2. Doxorubicin recovery

A DOX calibration curve was constructed using five concentrations from 10^{-8} *M* to 10^{-10} *M* plus a blank. The equation:

$$y = (1.4\pm0.04)\times 10^{-9}X - (0.18\pm1.3) \times 10^{-10}\ (r^2 = 0.9956),$$

where y is molar concentration, X is the peak area (arbitrary units), and r is the correlation coefficient, predict a linear dependence. The regression was linear over the concentration range of 10^{-8} *M* to 10^{-10} *M* DOX. Assuming that each metabolite has similar fluorescent properties, this calibration curve

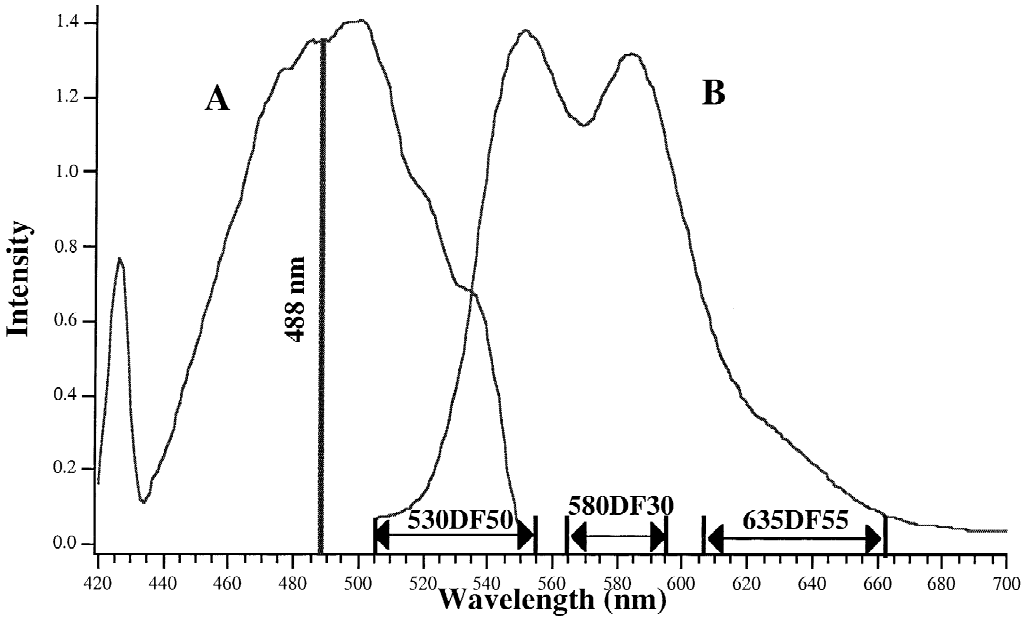

Fig. 2. The excitation and emission spectra of 10^{-7} *M* DOX in BS buffer. After determination of the excitation spectrum (A), the emission spectrum (B) was obtained using 488-nm excitation. The vertical line at 488 nm represents the wavelength of excitation used in LIF experiments. The spectral bandpass for the three filters discussed in this report are shown. Scale of excitation spectrum adjusted to match that of the emission spectrum.

helps to calculate the amounts of DOX or metabolite in a given sample.

Based on five independent liquid–liquid extractions of the same cell treatment, the recovery of DOX was 50±15, 77±16 and 99±20% for 1×10^{-7}, 1×10^{-8} and 1×10^{-9} *M* DOX, respectively. The large variation in recovery for a given concentration is common in procedures involving multiple step extractions. In addition, these data hint to a slight dependence of extraction efficiency with DOX concentration. The percent recovery for 1×10^{-9} *M* DOX is significantly different than that for 1×10^{-7} *M* DOX.

Furthermore, it is expected that the structural features in the metabolite molecule will affect their extraction. Loss of the daunosamine sugar (Fig. 1) would break the intramolecular hydrogen bond with the glycosidic oxygen and allow the hydroxyl group

Table 1
Optimization of doxorubicin detection

Filter[a]	530±22.5 (nm)	580±15 (nm)	635±27.5 (nm)
Collected fluorescence[b]	32	36	14
Background[c] (V)	0.143	0.725	0.0757
Noise[d] (V)	0.003	0.005	0.001
LOD[e] (zmol)	380±80	340±90	60±10

[a] The transmission range for the interference filter has been provided by the manufacturer (Omega Optical).

[b] Collected fluorescence is an estimate based on the area overlap of the doxorubicin emission spectra (Fig. 2) and the transmission range for the interference filter.

[c] The background is the average of the baseline of a typical electropherogram.

[d] The noise is the standard deviation of the baseline of a typical electropherogram.

[e] The limit of detection (LOD) is determined as the quantity of doxorubicin that produces a signal-to-noise ratio equal to three. The reported value is the average of three determinations done on different days.

at position 6 to be deprotonated. Therefore, deglycosilation would actually serve to increase the charge on the metabolites thus making extraction into the organic phase less efficient than the extraction of DOX. On the other hand, the conversion of DOX to doxorubicinol (DOXol) increases the hydrogen bond acidity of the molecule (Fig. 1). Therefore it is possible that the extraction of DOXol will be more efficient than the other metabolites due to increased hydrogen bonding with methanol in the extraction solvent.

3.3. Metabolite analysis in bulk

Fig. 3A, trace (i), is an electropherogram that results from treating 1.6±0.4 million NS-1 cells with 25 μ*M* doxorubicin for 8 h. The extract of untreated NS-1 cells was used as a control, (Fig. 3A, trace (iii)). The small peak at a migration time of 113 s is most likely due to methanol in the sample as it also appears in the controls. The peak is not in the metabolite migration window (150–300 s) and therefore does not pose any interference to the analysis.

In order to study the potential degradation of DOX during the extraction procedure, DOX was added to untreated cells just before the lysing and extracting steps. In this short contact time (~1 min) at room temperature it is unlikely that DOX would be metabolized. In the electropherogram of this extraction control, there is a second peak following the DOX peak (Fig. 3A, trace (ii)). Since DOX is stable in methanolic solution [19,39] the second peak is likely a degradation product resulting from the liquid–liquid extraction procedure. This second peak may have not been resolved in Fig. 3A, trace (i), due to the high level of DOX present in that sample. These results clearly indicate the need of extraction controls, the presence of unwanted transformations during the extraction procedure, and the risk of an incorrect interpretation of metabolism.

Excluding the artifacts caused during the extraction protocol, metabolite peaks (1, 2, 3, 5, and 6) in addition to the DOX peak were always detected (Fig. 3 and Table 2) in five independently prepared NS-1 extracts from the same DOX treatment. In comparison with previous reports, detection of additional metabolites is made possible by the high sensitivity of post-column LIF detection. Metabolite peaks 4 and 7–10 (Fig. 3 and Table 2) were not detectable in all replicates. This is likely to be an effect of slight changes in their mobility which causes overlapping with major metabolite peaks. It was also observed that the migration time of DOX increased after

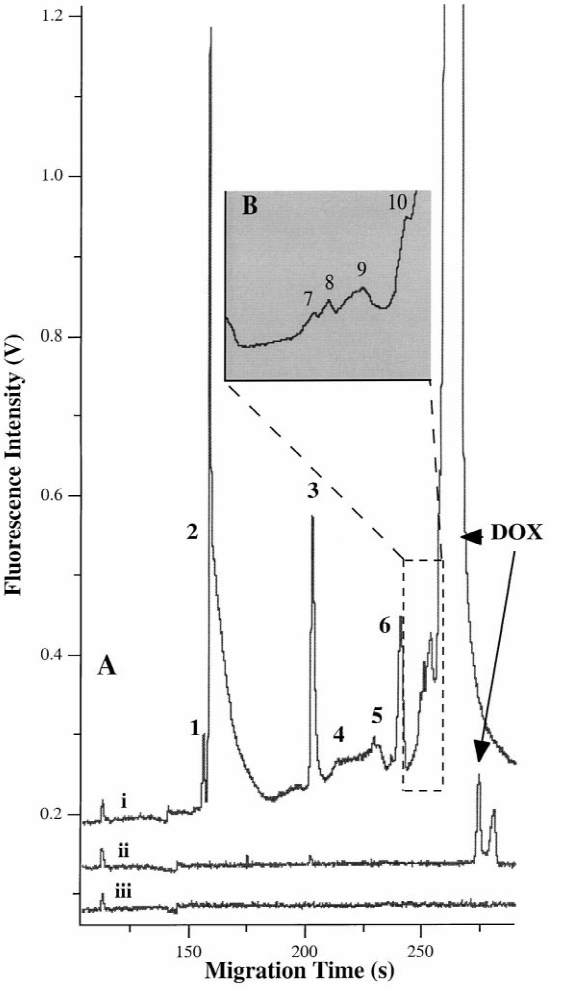

Fig. 3. Capillary electrophoresis separation of DOX and metabolites from a cell extract. Following NS-1 cells treated with 25 μ*M* DOX for 8 h, Trace A(i). Part B is an expansion to show peaks 7–10. Recovery control: 1×10^{-9} *M* DOX added to cell lysate of non-treated cells prior to extraction, Trace A(ii). Extraction control: Untreated NS-1 cells, Trace A(iii). Electrophoresis buffer was BS buffer. Separation performed in a 35.0 cm×50 μm I.D. fused-silica capillary, separation voltage of +403 V/cm following a 5-s injection using 100 V/cm. The 488-nm line of an argon-ion laser was used for excitation and a 635±27.5 nm bandpass filter was used for detection. Traces have been offset for clarity.

Table 2
Doxorubicin metabolites

Metabolite[a] ($n=5$)	Migration time (s)	Peak area[b]	Metabolite amount per cell[c] (amol)	Abundance[d] (%)
1	157±5	0.2±0.2	0.07±0.05	0.003±0.006
2	159±5	3.4±0.9	1.1±0.3	0.03±0.04
3	210±14	0.7±0.3	0.3±0.1	0.008±0.01
4[e]	220±13	0.3±0.2	0.1±0.07	0.004±0.005
5	240±15	0.4±0.2	0.2±0.1	0.004±0.006
6	250±15	0.6±0.2	0.3±0.1	0.006±0.008
7[f]	260	0.1	0.06	0.001
8[f]	245	0.06	0.03	0.0002
9[e]	270±19	0.3±0.1	0.1±0.08	0.001±0.004
10[f]	251	0.3	0.2	0.001
DOX	297±5	16 000±13 000	9500±7500	100

[a] Metabolite numbering system is the same as in Fig. 3. Data correspond to the average of five independent extractions and their corresponding CE–LIF analyses. Variation is represented as the standard deviation.
[b] Peak area is reported in arbitrary units.
[c] Metabolite amount was calculated from the average area, the calibration curve, and the total number of cells $1.6\pm0.4\times10^6$ cells per replicate.
[d] Relative abundance is calculated as percent of DOX peak area.
[e] Detected in four of the five replicates.
[f] Detected in two of the five replicates.

dilution of the sample, suggesting that other variations in migration time may result from capillary over loading with DOX, as it was necessary for detection of low-abundance metabolites. Also migration time variations may be caused by modifications of the capillary surface by cellular components that are co-extracted with DOX and its metabolites.

At the time this manuscript was written, aglycone metabolite standards were not commercially available. Therefore, identification of all of the DOX metabolites based on their migration time is not straightforward. For the DOXol standard the migration time is almost identical to a DOX standard or extracted DOX (data not shown). Thus DOXol produced by the metabolism of DOX in the NS-1 cells would not be detected because of overlap with the large parent drug peak (Fig. 3). For aglycones, their electrophoretic mobility in relation to DOX mobility is predicted based on two of their structural features: (i) they are smaller molecules than DOX or DOXol; and (ii) at pH 9.3 they have two deprotonated hydroxyl groups in positions 11 and 6 (Fig. 1) while DOX or DOXol have only one [36,40]. Based on these two features, the mobility of the aglycones is expected to be more negative than that of DOX or DOXol. Therefore in free zone electrophoresis, it is predicted that DOX will migrate faster than the aglycones. On the other hand, in micellar electrokinetic capillary chromatography, the separation mode used in this study, DOX and metabolite apparent mobility is also affected by partitioning between the micellar and aqueous phases. It is expected that the aglycones will partition less than DOX into the micelles due to the additional negative charge thus migrating faster than DOX. This speculation is consistent with the electropherogram in Fig. 3 which suggest that the components migrating earlier than DOX should correspond to aglycones.

On the other hand, the number of peaks in the metabolite electropherogram (Fig. 3A, trace (i)) exceeds the number of metabolites reported to date [13]. Likely other metabolites have not been previously reported because they have escaped detection. Another potential explanation is the presence of complex formation between phospholipids or proteins and DOX or metabolites altering their mobility. Further characterization or isolation of these unidentified peaks may lead to the discovery of novel drug–biomolecule interactions or to enhance the description of DOX metabolism.

The peak areas in Fig. 3 (Table 2) and in the calibration curve described above, facilitated to

calculate the average metabolite amount per cell and their relative abundance with respect to DOX. In all cases the DOX peak could not be obtained at the initial sample dilution, therefore the sample was further diluted 5000 to estimate its peak area. The average amount of doxorubicin per cell was 9.5 fmol/cell while the metabolites are found at levels between 0.03 and 1.1 amole per cell. These values are lower than those previously reported by Licata et al. [13] who used a closed enzymatic system. The accumulation of metabolites in a closed system is certainly expected to result in higher metabolite content than an open cellular system where metabolite excretion is a dynamic process.

3.4. Single cell analysis

After treatment with 25 μ*M* DOX for 8 h, one single NS-1 cell was introduced into the separation capillary, lysed with the BS running buffer, and then analyzed by CE–LIF. Fig. 4A is an electropherogram resulting from the analysis of a single NS-1 cell. This profile is not identical to that one resulting from a bulk extraction (Fig. 4B) but tentative assignments

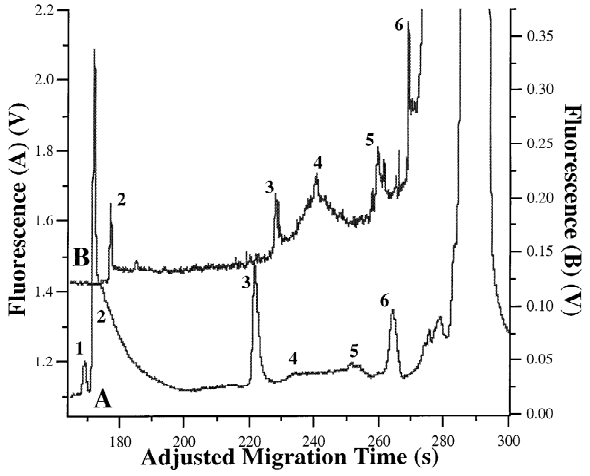

Fig. 4. Single NS-1 cell analysis compared to bulk cell extract metabolite separation. Single NS-1 cell treated with DOX (A). Cell extract from NS-1 cells treated with DOX (B). A suspension in mannitol buffer was introduced by a 1-s siphoning injection (11.2 kPa). Separation performed in a 39.5 cm×20 μm I.D. fused-silica capillary, separation voltage of +400 V/cm. Other conditions as in Fig. 2. Traces have been offset for clarity.

are still feasible. The origin of the variations in migration time and peak areas are discussed below.

Variations in the migration time may result from: (i) wall modifications resulting from the presence of cell components such as lipids and hydrophobic proteins co-extracted in bulk or all the cell components released during the lysis of a whole cell inside the capillary; (ii) overloading of the capillary with DOX in bulk analyses; and (iii) alterations in the zone field or wall modifications caused by the components in extra-cellular buffer introduced along with the cell in a single cell injection. Efforts to eliminate migration time bias are underway.

In contrast to the variations in migration time, the absolute and relative peak areas for each metabolite are expected to be different among individual cells and bulk extracts. Indeed analysis of multiple cells (25 cells) reveal that the metabolic profile for each cell is unique. Furthermore it is expected that: (i) there are no losses; and (ii) degradation is minimized in the single cell procedure. In agreement with this expectation the typical single cell analysis represented in Fig. 4B reveals that that cell contains 0.1, 0.3, 0.5, 0.2 and 1.1 fmol of metabolites 2, 3, 4, 5 and 6, respectively. In the bulk extraction analysis the amount of same metabolites were estimated to be at least 100-fold lower, which strongly warns users about testing the extraction efficiency of each component in a metabolite mixture. On the other hand, the use of single cell electropherograms may provide a more realistic scenario of metabolism in a given cell type.

3.5. Conclusions

We have successfully developed a method for the separation and detection of at least five DOX metabolites extracted from a cell culture. The high sensitivity and low limits of detection of post-column LIF makes it possible to detect up to ten DOX metabolites present at zmole per cell concentrations. Single cell analysis providing 100% recovery eliminates the need for recovery studies and decreases the risk of unwanted metabolite transformation during the extraction procedure in bulk. It is expected that the ability to separate and detect low levels of DOX and its metabolites will help in the early detection of unwanted metabolite formation and perhaps help to

identify more efficient and less deleterious chemotherapeutic regiments.

Acknowledgements

Financial support from the National Institute of Health (R01-GM61969-01A1) and the Office of the Vice President for Research and Dean of the Graduate School of the University of Minnesota (Grant-in-aid) is greatly appreciated. A.A. thanks NIH support through a Biotechnology Training Grant (#5-T32-GM08347). Dieter Starke, University of Alberta, for construction of the capillary holder used for single cell analysis. Kathyrn Fuller and Nilhan Gunasekera for maintenance of cell cultures. Dr Antonio Suarato, Pharmacia, for his kind donation of 13-dihydrodoxorubicin (doxorubicinol).

References

[1] G.N. Hortobagyi, Drugs 54 (1997) 1.
[2] D.J. Booser, G.N. Hortobagyi, Drugs 47 (1994) 223.
[3] M. Schwonzen, C.M. Kurbacher, P. Mallmann, Anticancer Drugs 11 (2000) 681.
[4] R. Woessner, Z. An, X. Li, R.M. Hoffman, R. Dix, A. Bitonti, Anticancer Res. 20 (2000) 2289.
[5] A. Bodley, L.F. Liu, M. Isreal, R. Seshadri, Y. Koseki, F.C. Giuliani, S. Kirschenbaum, R. Silber, M. Potmesil, Cancer Res. 49 (1989) 5969.
[6] P. de Bruijn, J. Verweij, W.J. Loos, H.J. Kolker, A.S.T. Planting, K. Nooter, G. Stoter, A. Sparreboom, Anal. Biochem. 266 (1999) 216.
[7] R. Jeyaseelan, C. Poizat, H. Wu, L. Kedes, J. Biol. Chem. 272 (1997) 5828.
[8] P.K. Singal, C.M. Deally, L.E. Weinber, J. Mol. Cell. Cardiol. 19 (1987) 817.
[9] S.F. Wadler, Z. Joachim, P.H. Wiernik, J. Clin. Pharm. 26 (1986) 491.
[10] N. Baldini, K. Scotland, M. Serra, T. Shikita, N. Zini, A. Ognibene, S. Santi, R. Ferracini, N.M. Maraldi, Eur. J. Cell Biol. 68 (1995) 226.
[11] M.R. Abbaszadegan, A.E. Cress, B.W. Futscher, W.T. Bellamy, W.S. Dalton, Cancer Res. 56 (1996) 5435.
[12] P.M. Sokolove, Int. J. Biochem. 26 (1994) 1341.
[13] S. Licata, A. Saponiero, A. Mordente, G. Minotti, Chem. Res. Toxicol. 13 (2000) 414.
[14] A. Andersen, D.J. Warren, L. Slördal, Cancer Chemother. Pharmacol. 34 (1994) 197.
[15] S. Nagaraj, H.T. Karnes, Biomed. Chromatogr. 14 (2000) 234.
[16] F. Lachâtre, P. Marquet, S. Ragot, J.M. Gaulier, P. Cardot, J.L. Dupuy, J. Chromatogr. B 738 (2000) 281.
[17] P.W. Buehler, S.J. Robles, G.R. Adami, R. Gajee, A. Negrusz, Chromatographia 49 (1999) 557.
[18] J. van Asperen, O. van Tellingen, J.H. Beijnen, J. Chromatogr. B 712 (1998) 129.
[19] G. Hempel, P. Schulze-Westhoff, S. Flege, N. Laubrock, J. Boos, Electrophoresis 19 (1998) 2939.
[20] J. De Jong, W.S. Guerand, P.R. Schoofs, J. Chromatogr. 570 (1991) 209.
[21] A. Andersen, D.J. Warren, L. Slördal, Ther. Drug Monit. 15 (1993) 455.
[22] C. Mou, N. Ganju, K.S. Sridhar, A. Krishan, J. Chromatogr. B 703 (1997) 217.
[23] P. Zhao, A.K. Dash, J. Pharm. Biomed. Anal. 20 (1999) 543.
[24] N.J. Reinhoud, U.R. Tjaden, H. Irth, J. van der Greef, J. Chromatogr. 574 (1992) 327.
[25] T. Perez-Ruiz, C. Martinez-Lozano, A. Sanz, E. Bravo, Electrophoresis 22 (2001) 134.
[26] G. Hempel, S. Haberland, P. Schulze-Westhoff, N. Mohling, G. Blaschke, J. Boos, J. Chromatogr. B 698 (1997) 287.
[27] N. Siméon, E. Chatelut, P. Canal, M. Nertz, F. Couderc, J. Chromatogr. A 853 (1999) 449.
[28] G. Chen, A.G. Ewing, Crit. Rev. Neurobiol. 11 (1997) 59.
[29] S.N. Krylov, D.A. Starke, E.A. Arriaga, Z. Zhang, N.W.C. Chan, M.M. Palcic, N.J. Dovichi, Anal. Chem. 72 (2000) 872.
[30] R.T. Kennedy, M.D. Oates, B.R. Cooper, B. Nickerson, J.W. Jorgenson, Science 246 (1989) 57.
[31] Q. Xue, E.S. Yeung, Anal. Chem. 66 (1994) 1175.
[32] A. Malek, M.G. Khaledi, Anal. Biochem. 270 (1999) 50.
[33] S.N. Krylov, Z. Zhang, N.W.C. Chan, E.A. Arriaga, M.M. Palcic, N.J. Dovichi, Cytometry 33 (1999) 15.
[34] S.N. Krylov, E. Arriaga, Z. Zhang, N.W.C. Chan, M.M. Palcic, N.J. Dovichi, J. Chromatogr. B 741 (2000) 31.
[35] C.F. Duffy, S. Gafoor, D. Richards, H. Ahmadzadeh, R. O'Kennedy, E.A. Arriaga, Anal. Chem. 73 (2001) 1855.
[36] G. Razzano, V. Rizzo, A. Vigevani, Il Farmaco 45 (1990) 215.
[37] J.R. Mazzeo, in: J.P. Landers (Ed.), Handbook of Capillary Electrophoresis, CRC Press, Boca Raton, FL, 1997, p. 49, Chapter 2.
[38] S. Wu, N.J. Dovichi, J. Chromatogr. 480 (1989) 141.
[39] F. Arcamone, G. Cassinelli, G. Fantini, A. Grein, P. Orezzi, C. Pol, C. Spalla, Biotechnol. Bioeng. XI (1969) 1101.
[40] L. Kleeberger, E.M. Rottinger, Cancer Chemother. Pharmacol. 33 (1993) 144.